POST-STACK DIP- AND AZIMUTH PROCESSING

KRISTOFER M. TINGDAHL[1] and PAUL F.M. DE GROOT[2]

[1] *Department of Earth Sciences-Marine Geology, Göteborg University, Box 460, SE-405 30 Göteborg, Sweden.*
[2] *dGB Earth Sciences, Boulevard 1945-24, NL-7511 AE Enschede, The Netherlands.*

(Received April 8, 2003; revised version accepted May 19, 2003)

ABSTRACT

Tingdahl, K.M. and de Groot, P.F.M., 2003. Post-stack dip- and azimuth processing. *Journal of Seismic Exploration*, 12: 113-126.

This paper describes background and applications of post-stack dip- and azimuth processing. Our workflow starts with the creation of a "steering-cube", i.e., a volume that contains seismic dip- and azimuth information at every sample position. From the steering cube we derive a number of interesting attributes. In this paper we present the variance of the dip as a valuable indicator for capturing chaotic reflection patterns. We also show how the steering cube enables us to derive curvature attributes at every sample position in a volume. These attributes are used a/o to detect faults and subtle stratigraphic features. Without the benefit of a steering cube, curvature attributes can only be calculated along mapped horizons.

Another application of the steering cube is its use to extract information from the original seismic volume along local reflector orientations. This "dip-steering" process can be used to filter data and to extract volume attributes. In this paper we will discuss dip-steered, edge-preserving smoothing filters that remove non-coherent noise and enhance laterally continuous events without introducing filter-tails at event edges. Similarity is presented as an example of a dip-steered volume attribute. To show the importance of dip-steering we compare similarity with and without dip-steering. All presented example applications show the value and versatility of the steering cube.

KEY WORDS: dip-steering, edge-preserving smoothing, attributes, filters.

0963-0651/03/$5.00

INTRODUCTION

Dalley et al. (1989) are credited for introducing dip and azimuth calculations along mapped horizons. In the last decade, various algorithms were introduced to calculate dip- and azimuth at every sample position (e.g., Steeghs, 1997; Tingdahl, 1999, 2003). The articles on coherency (e.g., Bahorovich and Farmer, 1995) initially focussed on the use of coherency as an interpretation attribute but it was soon realised that dip and azimuth, a by-product of the more advanced coherency algorithms, could also be used to extract seismic attributes (Marfurt et al., 1998). Höcker and Fehmers (2002) presented filtering along seismic events as another application of dip- and azimuth processing. Within Shell their structure-oriented, edge-preserving filter has become a workhorse in many operating units they claim.

In our work with seismic object detection (Meldahl et al., 1999; Tingdahl, 2003), dip-azimuth processing is a key element of the detection scheme. At the start of any project we calculate a "steering cube" containing dip- and azimuth information at every sample position. The steering cube is subsequently used to guide filters and attribute extraction windows.

STEERING CUBE AND DIP-STEERING

Steering cube

Dip and azimuth can be calculated in different ways. Coherency-based algorithms calculate some form of semblance in different directions. The direction with the highest semblance gives the dip and azimuth of the seismic event. Steeghs (1997) computes dip and azimuth from local slant stacks of the power spectra, a technique he refers to as 'Wigner-Radon transformation'. Tingdahl (2003) uses a 3D Fourier transform to find the local direction. This algorithm is computationally intensive (Table 1) but produces a stable dip- and azimuth. Fig. 1 shows one inline with the corresponding dip (Fig. 2a), which is a derivative from the calculated 3D dip- and azimuth. The dip- and azimuth

Table 1. Dip calculation benchmark. The test was performed on a Dual Intel Pentium 2.2 GHz computer.

Algorithm	Speed (samples per second)
Gradient	89,900
FFT based (cubesize 5×5×5)	12,100
FFT based (cubesize 7×7×7)	4,800

were calculated at every position by transforming a sub-cube of $7 \times 7 \times 7$ samples to the 3D Fourier domain and finding the maximum with the help of a third-order polynomial curve-fitting algorithm (Tingdahl, 2003). The algorithm fits a third-order, three-dimensional polynomial to a subcube around the sample of the highest energy in the Fourier domain. That polynomial is then searched for its local maxima, and the dip and azimuth corresponding to that local maxima is set as output.

If computational speed is an issue, we sometimes apply a much faster algorithm to compute a steering cube. This algorithm is based on two separate two-dimensional gradient calculations yielding an inline dip and crossline dip value. Fig. 2b shows the dip that follows from a 3-points horizontal gradient divided by a 3-points vertical gradient. Compared to the Fourier-based algorithm the dip is less accurate and noisier. Optionally applying a median smoothing filter to the calculated steering cube reduces the noise.

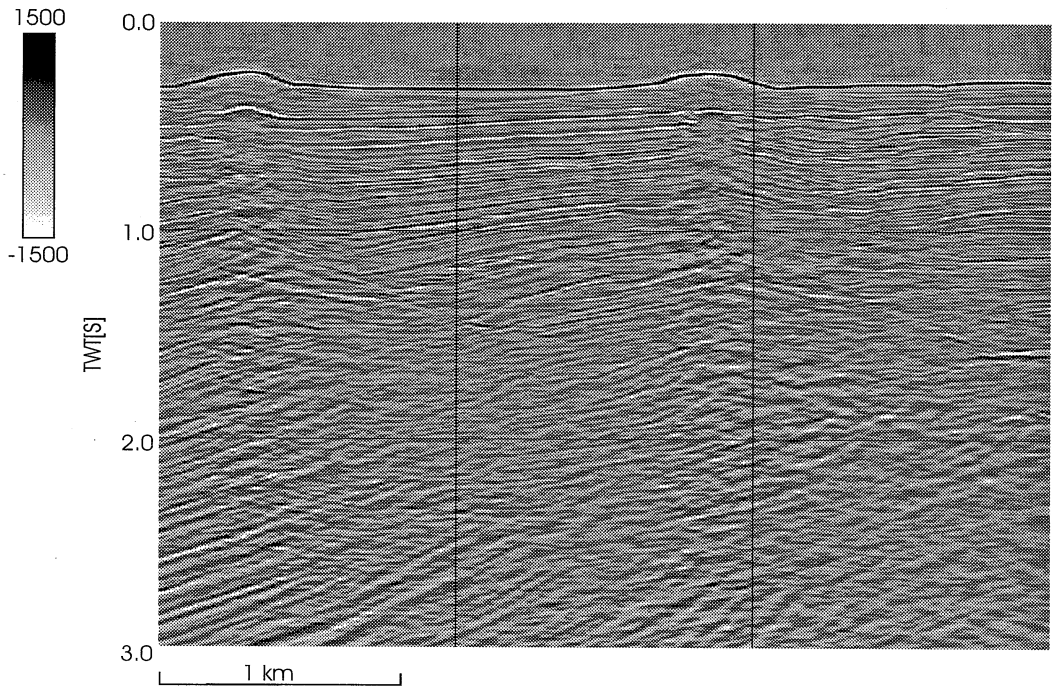

Fig. 1. Seismic inline.

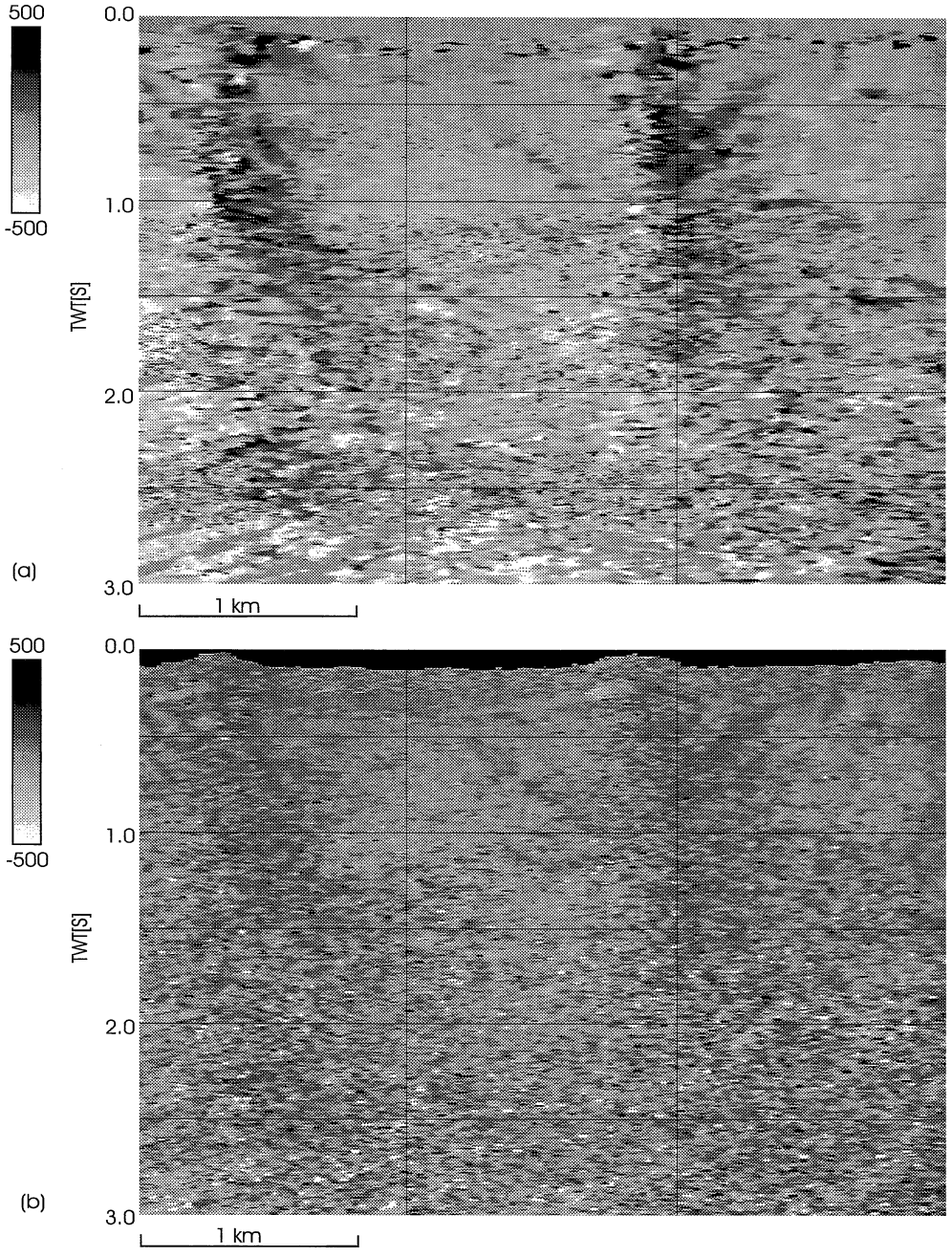

Fig. 2. Comparison of two dip-azimuth calculation algorithms computed from the inline in Fig. 1.- (a) corresponding dip calculated with the 3D Fourier-based algorithm using the 7×7×7-sub-cube and (b) corresponding dip calculated with a 3×3 gradient algorithm. The dip is given in microseconds per meter.

Auto-adaptive dip-steering

The essence of auto-adaptive dip-steering is that the seismic event is tracked in a search area around the evaluation point using local dip and azimuth information only. At each trace we compute the intersection of the search path and the trace (Fig. 3a). Optionally, an interval centred at the intercept time can be searched for the same phase as the phase of the starting position. The intercept time is then adjusted to the time of equal phase; a technique we call phase locking (Fig. 3b). At the (optionally phase locked) intercept time, the local dip and azimuth are followed to the next trace along the path and so on (Fig. 3c). Tracking an event in this way depends on the search path that must visit all trace positions within the search area. Fig. 4 shows the tracking scheme we use.

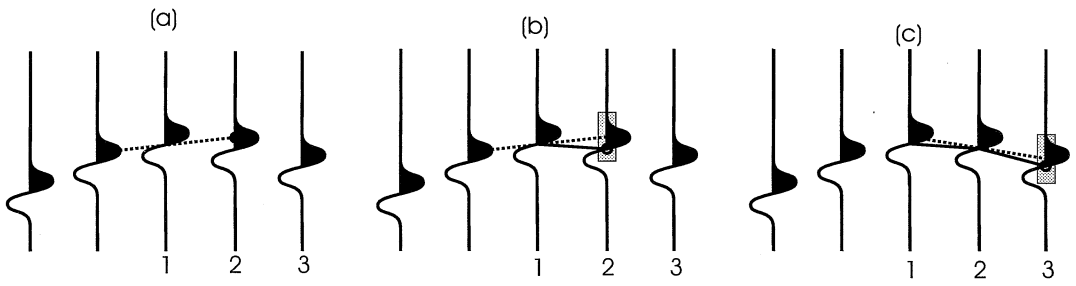

Fig. 3. The process of auto-adaptive dip-steering from trace one to trace three. Dashed lines represent the local dip and azimuth; solid lines between the traces represent the steering path (a) The local dip and azimuth are followed from one trace to the next. (b) Optionally, an aperture centred on the intercept time (grey-shaded interval) can be searched for the same phase as the phase at the starting position. If the phase is found within the aperture, the time is adjusted to the time of equal phase. (c) The local dip and azimuth at the (optionally phase adjusted) intercept time is retrieved from the steering cube and the process is repeated for the next trace until the target trace is reached (after de Rooij and Tingdahl, 2002).

APPLICATIONS

In the following examples, dip- and azimuth were all calculated with the 3D Fourier-based algorithm using the 7×7×7-sub-cube. The information is stored in the steering cube in the form of inline dip and crossline dip. Filters and attributes access the seismic volume and the steering cube simultaneously to process the data.

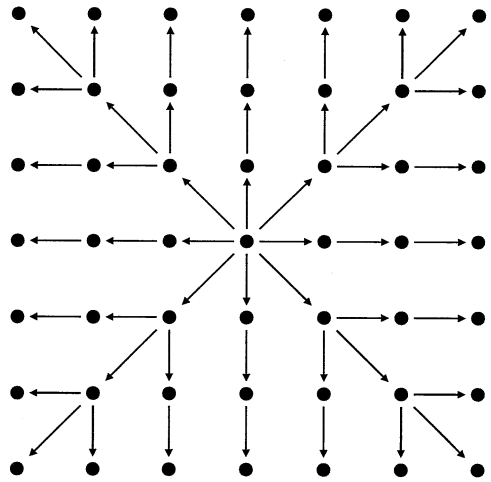

Fig. 4. Seismic traces seen from above. The auto-adaptive dip-steering technique travels from the source trace to the target trace via intermediate traces. The algorithm will move one inline/crossline position to the target trace at the time. Application of these rules yield the travel scheme shown.

Dip-steered edge-preserving filters

The aim of edge-preserving smoothing filters is to enhance lateral continuity of seismic events without distorting edges in the data. Non-coherent noise will be reduced and seismic (auto-)trackers generally perform better on filtered data (Höckers and Fehmers, 2002). In this section we describe and compare two dip-steered edge-preserving filters.

Dip-steered median filter

The median of a collection of values is defined as the value at the central position of the ranked values. So, if we rank all N amplitudes from smallest to largest number than we find the median by taking the value at position $(N+1)/2$, where N is an odd number. To understand the effect of a median filter, let us assume we are filtering a seismic event with a 3-point median filter. Let the event, i.e., the amplitude values along a horizon, be given by the following series:

...0,0,1,0,0,1,1,3,1,0,1,1,1,...

The 3-points median filtered response is then:

...0,0,0,0,0,0,1,1,1,1,1,1,1,1,1,...

To check this, take three consecutive input numbers, rank them and output the value in the middle, then slide your input set one position and repeat the exercise.

From this example we learn that:

* events smaller than half the filter length are removed (e.g., the 1 on the left and 0 on the right)

* noise bursts are also removed (the value 3) and

* edges are preserved (the break from mainly zeros to mainly ones stays exactly in the same position. In other words no filter tails are introduced).

Fig. 5 shows the effect of a dip-steered median filter with a radius of 4 traces, which corresponds to a 57-points median filter.

Dip-steered edge-preserving smoothing

Yi Luo et al. (2002) describe an edge-preserving filter that is based on a statistical analysis of the data around the evaluation point. The variance of the amplitudes extracted in a disk around the position is computed. This is done for all positions within a specified search radius around the evaluation point. The output of the filter is the average amplitude in the disk with lowest variance. The rational behind this approach is that the data will be locally disturbed at the edges. Hence, the variance of the amplitudes at these positions will be a high. Directly averaging the data at these positions will lead to smearing. Instead we will therefore substitute this unwanted average value with an average calculated at a position where the data is clean, i.e. away from the edges. Yi Luo et.al. (2002) do not use dip-steering when they apply their filter to coherency data. Given the low vertical resolution of coherency data dip-steering is not required. When applying the filter to enhance seismic data we must use dip-steering to extract amplitude information along the events instead of cutting through them.

Fig. 6 shows the edge-preserving smoothing filter dip-steering using a 4-trace search radius, which corresponds to 57-points.

Compared to the original seismic (Fig. 5a), both dip-steered filters have done a good job in reducing the non-coherent noise and enhancing the seismic events. The median filter appears to be smoother but edges are better preserved with the edge-preserving smoothing filter. However, the latter has introduced some unwanted jumps in previously continuous seismic events.

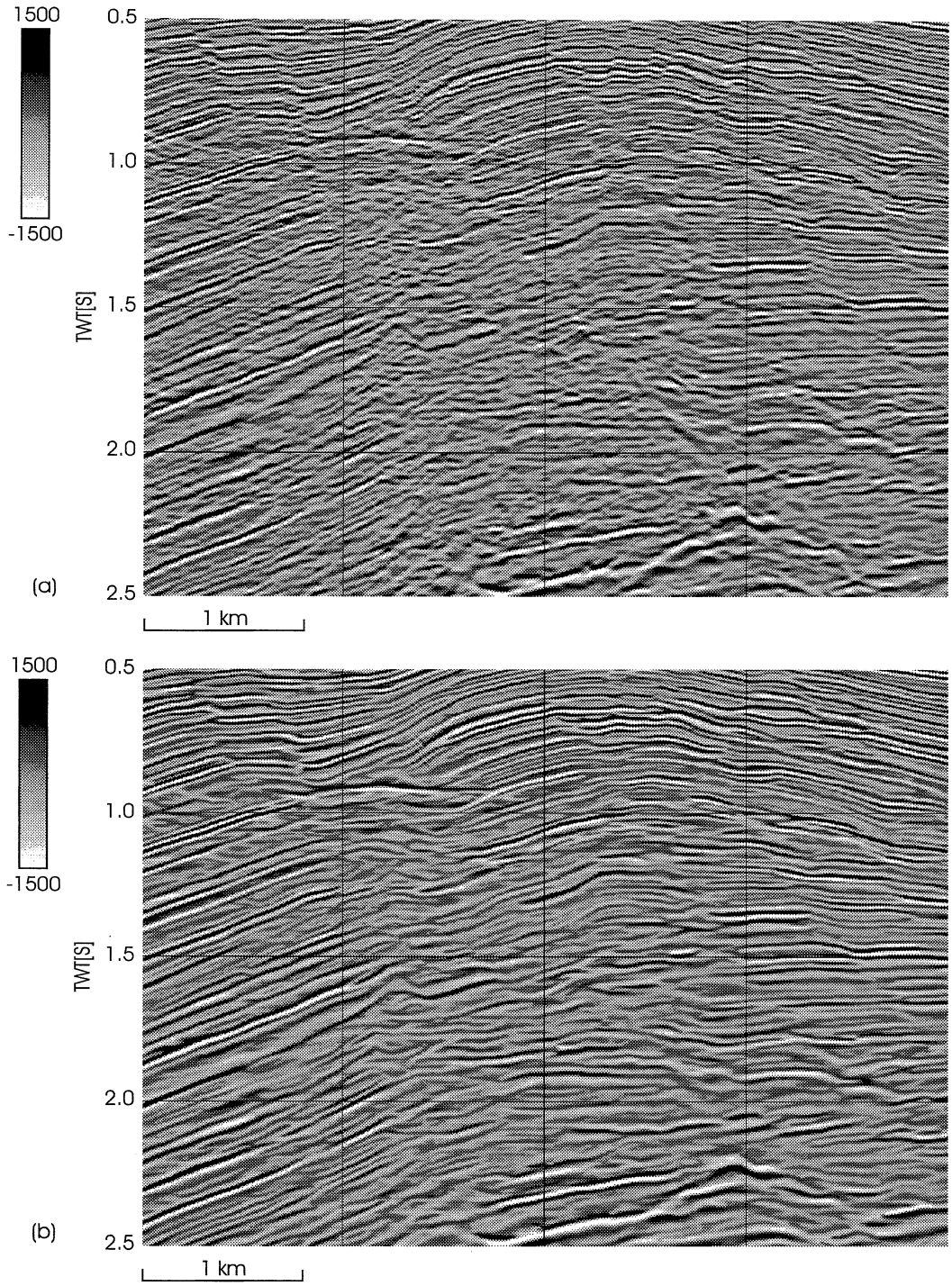

Fig. 5. (a) Seismic inline. (b) 57-points dip-steered median filter.

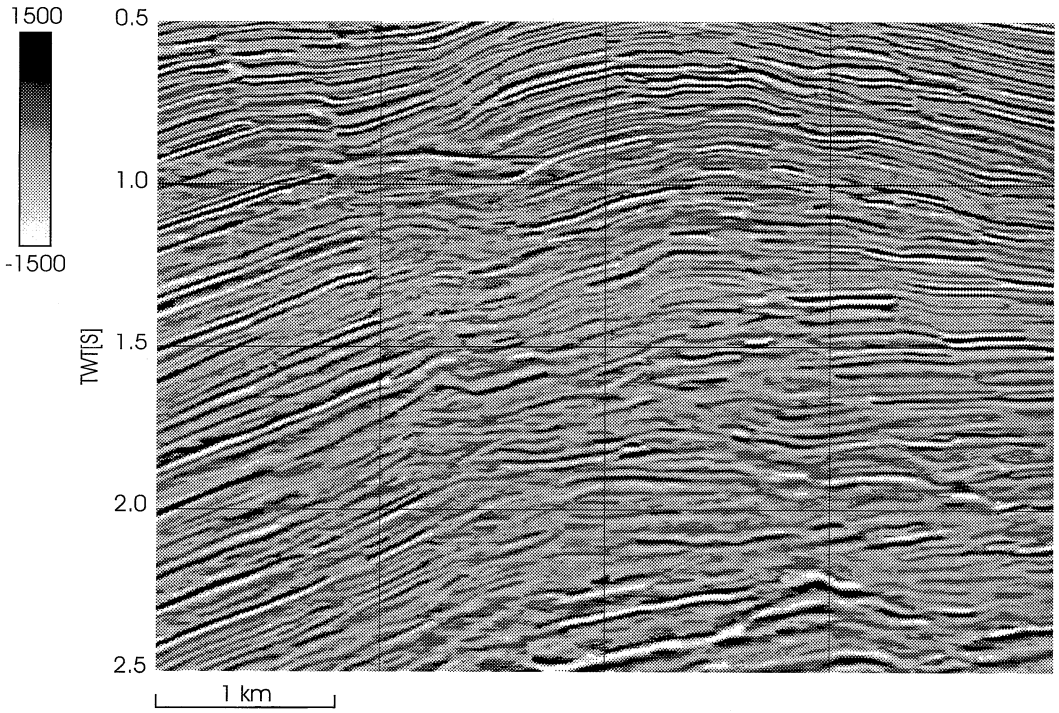

Fig. 6. 57-points dip-steered, edge-preserving smoothing filter (compare with Fig. 5).

Volume attributes

Volume attributes are defined as attributes calculated from multiple input traces. In this section we present three different volume attributes. The variance of the dip and the most positive curvature are attributes that are directly derived from the steering cube. Similarity is shown as an example of a dip-steered volume attribute.

Variance of the dip

The variance of the (polar) dip is calculated in a small sub-volume around the evaluation point. Fig. 7 shows the variance of the dip calculated in a 5x5x5 sample sub-volume. The attribute picks up chaotic reflection patterns. In the multi-attribute neural network-based object detection method developed by Meldahl et al. (1999) the variance of the dip is a key attribute for seismic chimney detection (Tingdahl, 2003).

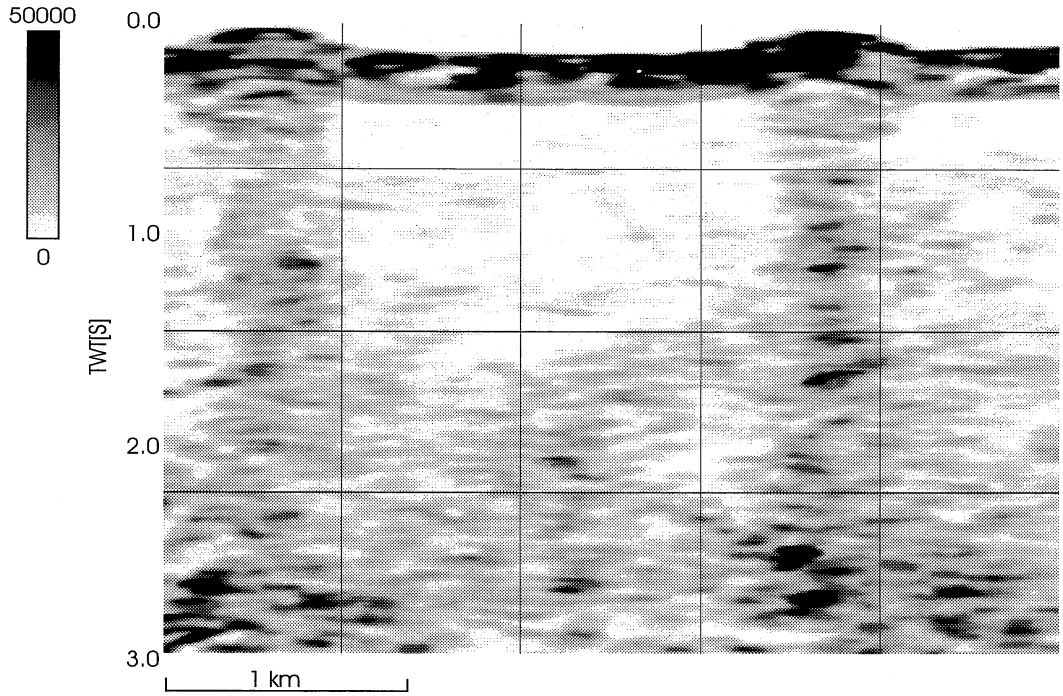

Fig. 7. Variance of the dip calculated in a 5x5x5 sample sub-cube from the inline in Fig. 1.

Curvature

Roberts (2001) defines curvature as a two-dimensional property of a curve that describes how bent a curve is at a particular point in the curve, i.e. how much the curve deviates from a straight line. The same concept is used to describe the curvature of a surface. Curvature is measured on the curve that is the intersection between a plane and the surface. Since this can be done in numerous ways there is an infinite number of curvature attributes that can be calculated for any plane. We use a subset of curvatures that is defined by planes that are orthogonal to the surface and which is called normal curvatures. To calculate curvature attributes a horizon, or part thereof, is a pre-requisite. Dip-steering is used to automatically construct a virtual horizon element at the evaluation point.

Fig. 8 shows the most-positive curvature as an example of curvature attributes. The most positive curvature returns the most positive curvature value from the infinite number of normal curvatures that exist. The attribute reveals

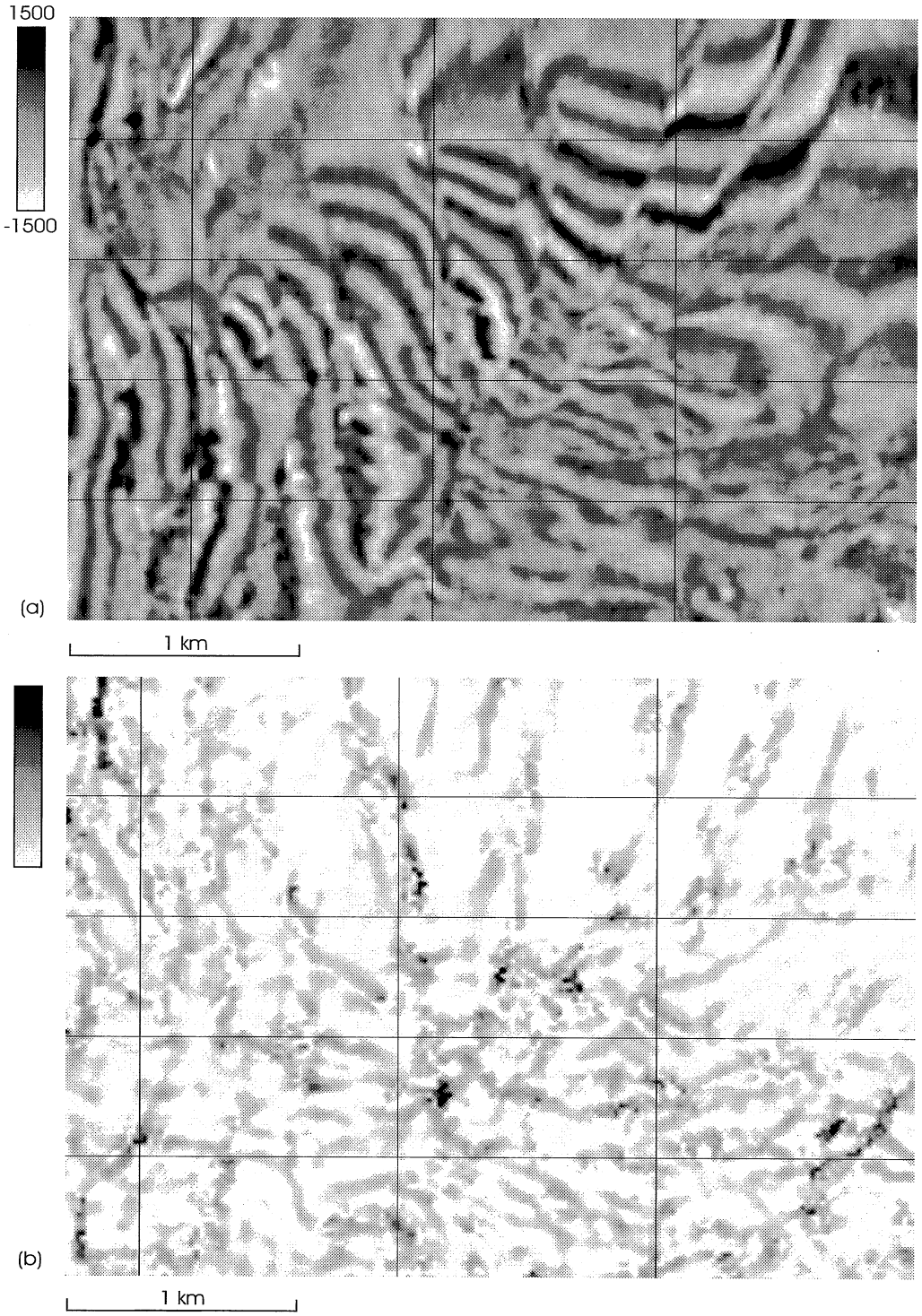

Fig. 8. (a) Seismic time-slice. (b) Most-positive curvature calculated from the steering cube using auto-adaptive dip-steering to compute local horizons at every sample position.

faulting and lineaments (Roberts, 2001). The magnitude of the lineaments is preserved but the shape information is lost. This attribute can be compared to first derivative based attributes (dip, edge and azimuth).

Similarity

Similarity is a form of "coherency" that expresses how much two or more trace segments look alike. Consider the samples of trace segments to be co-ordinates of vectors in hyperspace. Similarity is then defined as the Euclidean distance between the vectors, normalized over the vector lengths. A similarity of one means that the trace segments are completely identical in both waveform and amplitude. A similarity of zero means they are completely dissimilar. The trace segments to be compared are found by dip-steering. When more than 2 trace segments are compared the output is a statistical property, such as average, maximum, minimum or median, of the calculated similarities.

Fig. 9 shows a time-slice comparison between similarities computed with and without dip-steering. Both similarities were calculated by averaging an inline and crossline trace pair centred on the evaluation position. The used time-window is 40 ms (+ and − 20 ms). The comparison clearly shows that the dip-steered similarity (Fig. 9b) exhibits much greater detail than the non dip-steered similarity.

CONCLUSIONS

We presented a workflow for dip- and azimuth processing and showed various applications. The workflow started with the generation of a steering cube, a volume that contains the local direction of the seismic event at every sample position. Through the process of dip-steering we were able to apply edge-preserving filters. We presented the dip-steered median filter and the edge-preserving smoothing filter. Both filters removed non-coherent noise and enhanced laterally continuous events. The edge-preserving smoothing filter preserved edges better than the dip-steered median filter but it also introduced some unwanted jumps in the reflectors.

We also presented examples of volume attributes. The variance of the dip was shown as an example of an attribute that was directly derived from the steering cube. The attribute picked up chaotic seismic reflection patterns and has proven to be useful in multi-attribute seismic chimney detection. The most positive curvature was shown as an attribute that picks up small-scale faults and fault lineaments. Conventionally curvature attributes could only be calculated along mapped horizons. Dip-steering enabled us to construct a local horizon element at every sample position, which allowed to compute curvature attributes

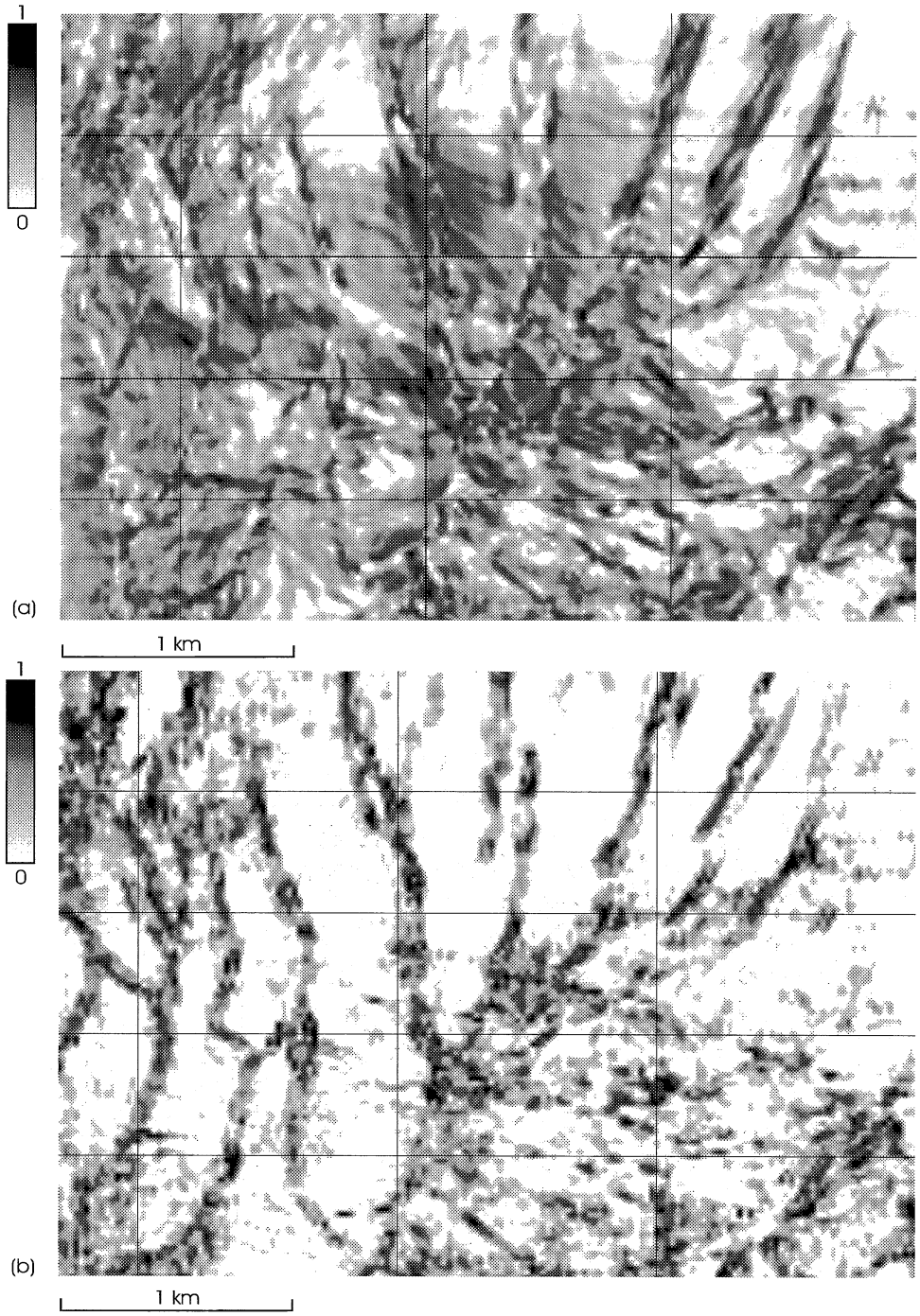

Fig. 9. (a) Similarity calculated from the data in Fig. 8a by averaging an inline and crossline trace pair centered on the evaluation position. A horizontal time-window of + and − 20 ms is used (i.e., no dip-steering is used). (b) Same as before with auto-adaptive dip-steering applied.

in a cube. Finally, we showed how similarity calculations improved through dip-steering.

All these example applications show the value and versatility of the steering cube. We believe that many more dip-steering applications will emerge in the near future. For example; we are working on seismic auto-trackers that will make full use of dip-steering capabilities. Such trackers will be able to cross through bad data zones.

ACKNOWLEDGEMENTS

Statoil, Göteborg University and dGB Earth Sciences have collaborated in the development of these techniques. The Royal Society of Sciences, Sweden is thanked for economical support to this study.

REFERENCES

Bahorich, M. and Farmer, S., 1995. 3-D seismic discontinuity for faults and stratigraphic features; the coherence cube. The Leading Edge, 14: 1053-1058.

Dalley, R.M., Gevers, E.C.A., Stampfli, G.M., Davies, D.J., Gastaldi, C.N., Ruijtenberg, P.A. and Vermeer, G.J.O., 1989. Dip and azimuth displays for 3D seismic interpretation. First Break, 7: 86-95.

de Rooij, M. and Tingdahl, K.M., 2002. Meta-attributes - The key to multivolume, multiattribute interpretation. The Leading Edge, 21: 1050-1053.

Höcker, C. and Fehmers, G., 2002. Fast structural interpretation with structure-oriented filtering. The Leading Edge, 21: 238-243.

Lou, Y., Marhoon, M., Al Dossary, S. and Alfaraj, M., 2002. Edge Preserving Smoothing and applications. The Leading Edge, 21: 136-141.

Marfurt, K.J., Kirlin, R.L., Farmer, S.L. and Bahorich, M.S., 1998. 3-D seismic attributes using a semblance-based coherency algorithm. Geophysics, 63: 1150-1165.

Meldahl, P., Heggland, R., Bril, A.H. and de Groot, P.F.M., 1999. The chimney cube, an example of semi-automated detection of seismic objects by directive attributes and neural networks. Part I: methodology. Expanded Abstr., 69th Ann. Internat. SEG Mtg., Houston: 931-934.

Roberts, A., 2001. Curvature attributes and their application to 3D interpreted horizons. First Break, 19: 85-100.

Steeghs, T.P.H., 1997. Local Power Spectra and Seismic Interpretation. Ph.D. thesis, Delft University of Technology.

Tingdahl, K.M., 1999. Improving seismic detectability using intrinsic directionality. M.Sc. thesis, Göteborg University.

Tingdahl, K.M., 2003. Improving seismic chimney detection using directional attributes. In: Nikravesh, M., Aminzadeh, F. and Zadeh, L.A. (Eds.), Soft Computing and Intelligent Data Analysis in Oil Exploration. Developments in Petroleum Science, 51: 157-173. Elsevier Science Publishers, Amsterdam.